Glacier changes in the Big Naryn basin, Central Tian Shan

W. Hagg [a,*], C. Mayer [b], A. Lambrecht [c], D. Kriegel [d], E. Azizov [e]

[a] Department of Geography, Ludwig-Maximilians-University, Luisenstr. 37, 80333 Munich, Germany
[b] Commission for Geodesy and Glaciology, Bavarian Academy of Sciences and Humanities, Alfons-Goppel-Str. 11, 80539 Munich, Germany
[c] Institute for Meteorology and Geophysics, University of Innsbruck, Innrain 52, 6020 Innsbruck, Austria
[d] Hydrology Section, GeoForschungsZentrum, Telegrafenberg, 14473 Potsdam, Germany
[e] Central Asian Institute for Applied Geosciences, Timur Frunze rd. 73/2, 720027 Bishkek, Kyrgyzstan

ABSTRACT

A glacier inventory referring to the year 2007 was created for the Big Naryn basin based on satellite imagery. The 507 glaciers had a total area of 471 km². Compared to the Soviet glacier inventory based on data from the mid 20th century, the total glacier area decreased by 23.4%. The shrinkage varies from 14% to 42% between individual mountain ranges. We discuss the possible causes for this considerable variation by analyzing and interpreting topographic parameters and differences between seven sub-regions.

On three glaciers, ice thickness was derived by ground penetrating radar (GPR) measurements on the glacier tongues and by surface slope using a simplified ice mechanical approach on the upper parts. We estimate the total ice volume of the basin for both inventories using volume–area scaling. Our results show a current glacier volume of 26.0–33.3 km³. A total of 6.6–8.4 km³ (20%) have been lost since the mid 20th century. The water equivalent of 5.9–7.6 km³ was transformed into excess discharge and contributed to at least 7.3–9.2% of total runoff in the considered period.

© 2012 Elsevier B.V. All rights reserved.

1. Introduction

Mountain glaciers are recognized as key indicators for climate change (IPCC, 2007) and as important water storages on a seasonal, mid-term and long-term time scale. Together with ice caps outside Greenland and Antarctica, they contain a sea level equivalent between 0.241 ± 0.026 m (Raper and Braithwaite, 2006) and 0.41 ± 0.03 m (Radić and Hock, 2010). Using a regionally differentiated glacier model, Van de Wal and Wild (2001) estimated that during the next 70 yr, Central Asia will have the largest contribution (0.018 m or 31%) to sea level rise of all glacier regions they considered. Several studies based on remote sensing have shown that glacier recession in Central Asia was accelerated during the past decades (Liu et al., 2006; Aizen et al., 2007; Bolch, 2007; Li et al., 2007), especially those at the outer ranges of the mountain systems (Narama et al., 2009). For the water cycle of the Central Asian mountains, glacier retreat will still be of crucial importance during the next century. Although the mean fraction of glacier melt in river discharge quickly decreases downstream (Weber et al., 2010), it still has high impact during dry periods in summer, when it is often the only runoff source additional to groundwater. This importance increases when the mountains are surrounded by arid lowlands, where irrigation during the vegetation periods often strongly depends on glacier melt (Kaser et al., 2010). These conditions can be found in the Syr-Darya basin, where the runoff generated in glacierized basins drains into steppes and deserts. The runoff formed in this basin is used for hydropower generation in the Toktogul reservoir in Kyrgyzstan and further downstream for irrigation in Uzbekistan. These seasonal differences in water demand imply a certain conflict potential along this transboundary river (e.g. Allouche, 2007; ECE, 2011).

The only glacier inventory which covers the whole basin is the Soviet Catalogue of Glaciers (Katalog Lednikov SSSR,1977), from here on referred to as "Katalog Lednikov", which is based on airborne imagery from the middle of the 20th century. To assess the changes since that period, we compiled a new glacier inventory from satellite imagery from 2007.

For future predictions of glacier areas and melt water yield, the volume of glaciers is required. Such data is generally rare, because it involves geophysical measurements which are time and labor intensive. Some studies (e.g. Haeberli and Hoelzle, 1995; Farinotti et al., 2009; Linsbauer et al., 2009) consider the principles of ice flow mechanics and derive ice thicknesses from the glacier surface topography. This is possible, because in principle the glacier surface represents a smoothed copy of its bed. Steeper and more rapidly flowing parts are thinner than flat parts with lower flow velocities. Based on earlier works (Erasov, 1968; Macheret et al., 1988; Chen and Ohmura, 1990), Bahr (1997) derived power-law scaling

* Corresponding author. Tel.: +49 89 2180 6657; fax: +49 89 2180 16503.
  E-mail addresses: hagg@lmu.de (W. Hagg), christoph.mayer@kfg.badw.de
(C. Mayer), Astrid.Lambrecht@uibk.ac.at (A. Lambrecht),
david.kriegel@gfz-potsdam.de (D. Kriegel), e.azisov@caiag.kg (E. Azizov).

relationships between the steady state volume of a glacier and its area. Although these relationships depend on the mass balance profile and may change with the state of a glacier, observations (Macheret et al., 1988; Meier and Bahr, 1996) show that it also delivers reasonable results for non-steady state conditions. Van de Wal and Wild (2001) and Radić et al. (2007) could show that results from volume–area scaling agree well with flowline modeling for future projections of the ice volume, although Radić et al. (2008) conclude that volume–length scaling is even a better approach.

We combine field measurements and considerations of ice flow to determine the volume of three selected glaciers in the Big Naryn basin, Central Tian Shan. This information allowed us to confirm the parameters of a volume–area scaling relation (Bahr, 1997) and enables us to estimate total ice volumes of the basin for the Katalog Lednikov (mid 20th century) and for the new 2007 inventory.

2. Hydrometeorological description of the investigation area

The Naryn River is formed at the confluence of the Big and the Small Naryn rivers. It flows into Ferghana Valley, where it merges with Kara-Darya to form the Syr-Darya River. We focus on the Big Naryn subbasin, which provides half of the long-term discharge at the estuary and contains the largest glacier areas. The catchment covers 5570 km² and stretches from 2260 m a.s.l. to 5112 m a.s.l. The watershed is formed by the Dzhetim and Dzhetimbel ranges and the Terskey-Alatau in the north, the Akshiirak massif in the east and by the Borkoldoy and Naryntau ranges in the south (Fig. 1).

The meteorological station "Tian Shan" near Petrov glacier in the northeastern part of the catchment (see Fig. 1) provides long-term records (since 1930) of temperature and precipitation from a high altitude location (3614 m a.s.l.). In 1997, the station was moved to a nearby site which is 46 m higher than the previous. Cross-correlations during a short period of overlapping measurements indicate good agreement for air temperature, but significant deviations for precipitation (Kutuzov and Shahgedanova, 2009). Therefore, precipitation data after 1997 was excluded from the analysis. Fujita et al. (2011) found that annual precipitation and summer (JJA) temperatures are the most crucial parameters for the glacier mass budget of the Gregoriev Glacier, which is located in the Big Naryn catchment. Between 1943 and 1997, annual precipitation decreases with a rate of 21.2 mm (4.3% of the mean value) per decade. Summer temperatures show a distinct increase between 1943 and 2003 with a rate of 0.2 °C per decade and a peculiar synchrony with annual runoff (Fig. 2). Precipitation, temperature and runoff trends are enforced since the 1970s. Visual interpretations of running means revealed that the long-term trend of the meteorological parameters changed in 1972. In the runoff series, a trend change is also obvious, but the exact timing is more difficult to ascertain due to a data gap around 1970. The significance levels of the trends were determined with a Mann–Kendall test (Kendall, 1975). Except for summer temperature and total runoff in the periods before 1973, all trends (of the complete and split time series) are significant at the 90% level. The true slopes of the existing trends (β), calculated by Sen's nonparametric method (Sen, 1968), are given in Fig. 2. Both of the two meteorological trends, i.e. temperature increase and precipitation decrease, support a loss of glacier mass.

3. Data and methods

Two panchromatic SPOT images (acquired on 22 August 2007) with a ground resolution of 5 m cover the eastern and most heavily glaciated part of the investigated area. They were mosaicked and then orthorectified using elevation information from ASTER-GDEM
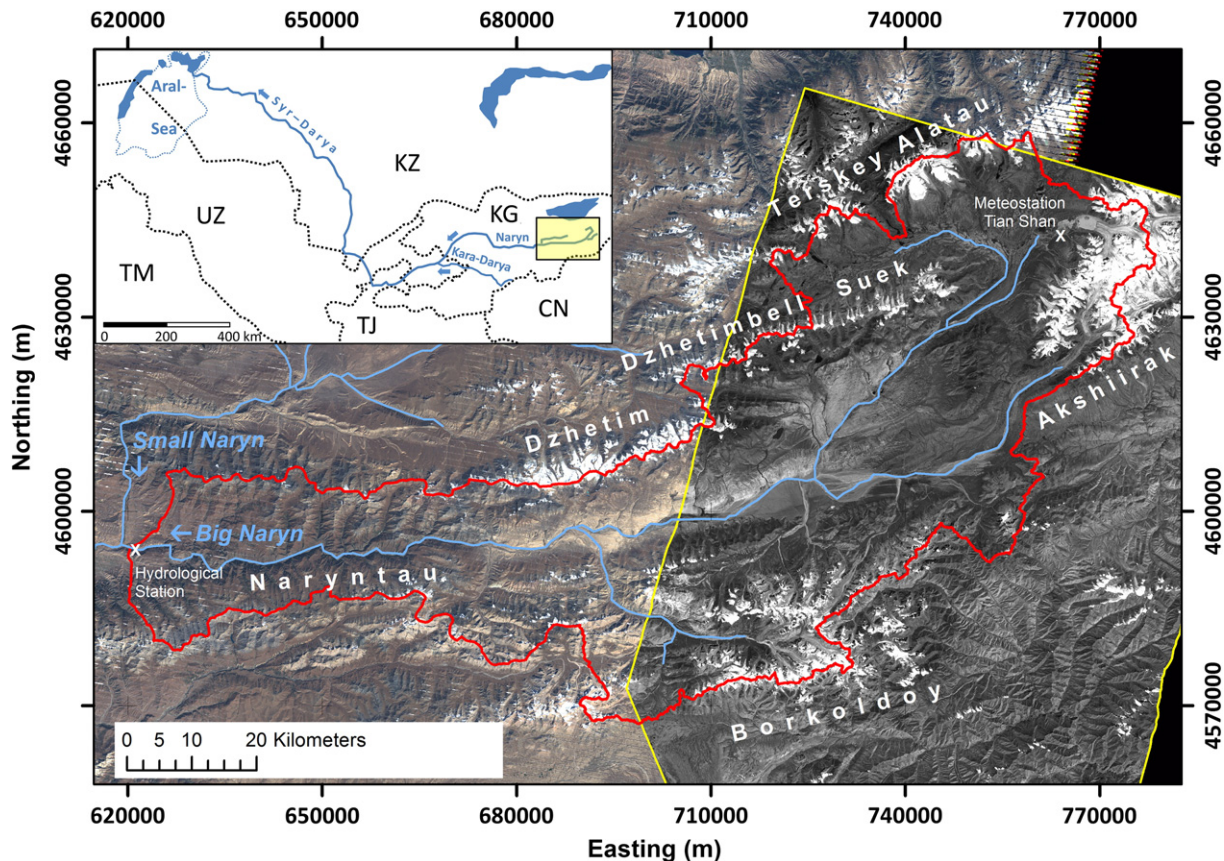

Fig. 1. Catchment of the Big Naryn (watershed in red) and location of the meteorological and hydrological stations on a pan-sharpened, multispectral Landsat image with 15 m resolution and a mosaic of 2 panchromatic SPOT scenes with 5 m resolution (yellow frame). Coordinate system: UTM, Zone 43. Country codes: CN—China, KG—Kyrgyzstan, KZ—Kazakhstan, TJ—Tajikistan, TM—Turkmenistan, UZ—Uzbekistan. (For interpretation of the references to color in this figure legend, the reader is referred to the web version of this article.)
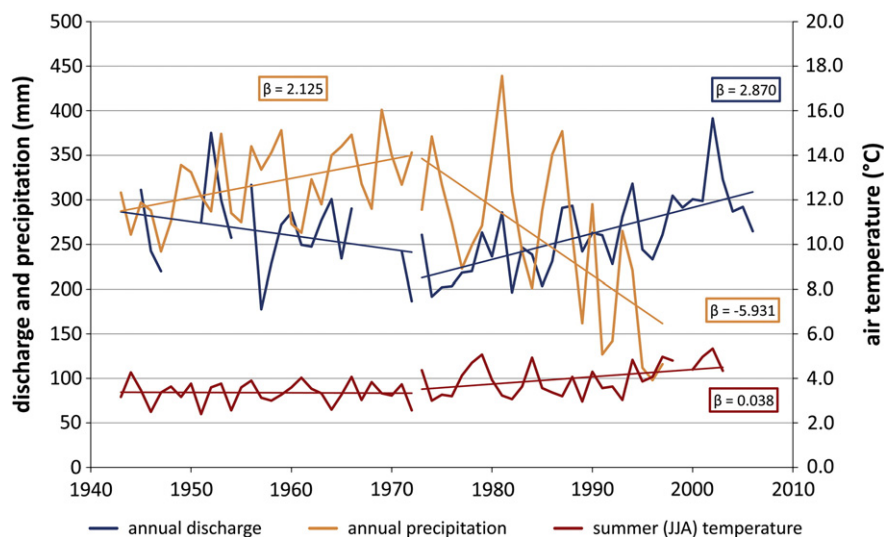
Fig. 2. Annual precipitation, summer (JJA) temperature of Tian Shan station (3614 m a.s.l., see Fig. 1) and annual discharge of Big Naryn. β-values are the true slopes of the existing trends calculated by Sen's nonparametric method (Sen, 1968).
Annual discharge data of Big Naryn from: Kyrgyz Hydromet.

(version 1, http://www.gdem.aster.ersdac.or.jp/), an elevation model with 30 m ground resolution and a product of METI and NASA. To delineate glacier boundaries, a grayscale mapping was performed in order to find a threshold which allows to detect glaciers automatically. The debris covered glacier parts could not be detected by this automatic approach and were digitized manually. In addition, snow patches which were classified as glaciers by the grayscale classification had to be identified and eliminated manually. Connecting glaciers were separated manually along the ice divide, which was visually traced using a hillshaded relief of the ASTER-GDEM.

The Landsat ETM image (acquired on 15 September 2007) was pan sharpened in a first step. This is a procedure to combine high resolution grayscale information with low resolution multispectral information. The result is an image with 15 m ground resolution and multispectral information, enhancing the visibility of small scale surface features. To fill data gaps caused by the scan line failure, we used an image from 17 September 2008 where the gaps are not at the same position. Many authors applied semi-automated multispectral glacier mapping, based on thresholding of ratio images (e.g. Paul and Kääb, 2005; Bolch and Kamp, 2006; Narama et al., 2009). Although this is a time efficient approach for large scale inventories, it requires manual corrections in many cases (Bolch et al., 2010). Considering the relatively small number and size of glaciers on the Landsat scene, we decided to map them manually on a false color composite (bands 5, 4, 3 as RGB). An example of the glacier mapping on both image types is given in Fig. 3.

Where glaciers are free from supraglacial debris, the glacier boundaries can be identified exactly on the images as the change in brightness from one pixel to another. However, an accuracy of one pixel remains due to the fact that they represent mean values and wrong classifications can occur on ice and rock surfaces. On the SPOT images, we estimate an accuracy of 2 pixels (10 m) due to the zoom level on which the mapping was performed, while on the Landsat scene a digitization with an accuracy of 1 pixel (15 m) was possible. To determine the error in glacier area, we created buffers of ±1 (Landsat) and ±2 (SPOT) pixels around our final glacier mask. The resulting deviations are +11%/−10% on the Landsat scene and +7.5%/−5.6% on the SPOT images. For the whole Big Naryn basin, the deviation from our mask is +7.9%/−6.2%.

Apart from very small patches that could easily be identified, snow is restricted to glacier areas on our late summer scenes and does not pose a problem. Debris covered glacier parts are the main sources of error for glacier mapping in our images. They can often be identified only indirectly. Convex morphological shapes, features which indicate movement or the uppermost point of the glacial stream can be hints on the glacier extent. On some glaciers in the Big Naryn catchment, the portion of debris covered areas and thus the potential error from an incorrect classification is as large as 25%. According to our visual interpretation, approximately 3.5% of the total glacier area is debris covered.

We used ASTER-GDEM data to delineate the watershed and to derive topographic features such as hypsographic curves, orientation distributions and surface slopes.

The glacier areas from the mid 20th century were taken from the Katalog Lednikov which is based on airborne photographs from 1943 (Akshiirak) and 1956 (all other regions). In the Naryntau, few glaciers were also pictured in 1959 (17%) and 1963 (9%) and in the Borkoldoy range, 41% of the glaciers were covered in 1959. The stable summer temperatures and slightly increasing winter precipitation from 1943 to 1956 make it unlikely that large glacier area changes occurred in that period. However, the different survey date for Akshiirak is considered in our areal analysis. The effect of the other temporal inconsistencies (1959 and 1963) can be neglected.

The GPR measurements were performed on three glaciers in the Suek range and in the Akshiirak massif (see Figs. 4 and 8) in July 2010 using a GSSI SIR 20 radar transmitter with a 200 MHz antenna. Tracks were recorded by GPS and analyzed using the Reflexw software. The point depths were interpolated using the topo2raster tool in ArcGIS, which is based on the ANUDEM program developed by Hutchinson (1993).Ice thicknesses from the upper glacier parts, where no measurements were carried out, were derived assuming simple shear and laminar flow as the only component of ice deformation (Paterson, 1994), as it is used for many approximations of simple glacier geometries (Eq. (1)),

$$h = \tau/(\rho \cdot g \cdot \sin \alpha) \cdot f \qquad (1)$$

where: h, ice thickness (m); τ, basal shear stress (kPa); ρ, density of ice (910 kg/m³); g, gravity acceleration (9.81 m s⁻²); α, surface slope (°); and f, shape factor.

Basal sliding can be neglected due to the cold conditions of the glacier ice in this region. A cold based glacier bed can be assumed regarding the mean annual temperature (1943–2003) of −7.6 °C recorded at the Tian Shan station. Moreover, our radargrams show an extremely weak internal structure, as it is typical for cold ice
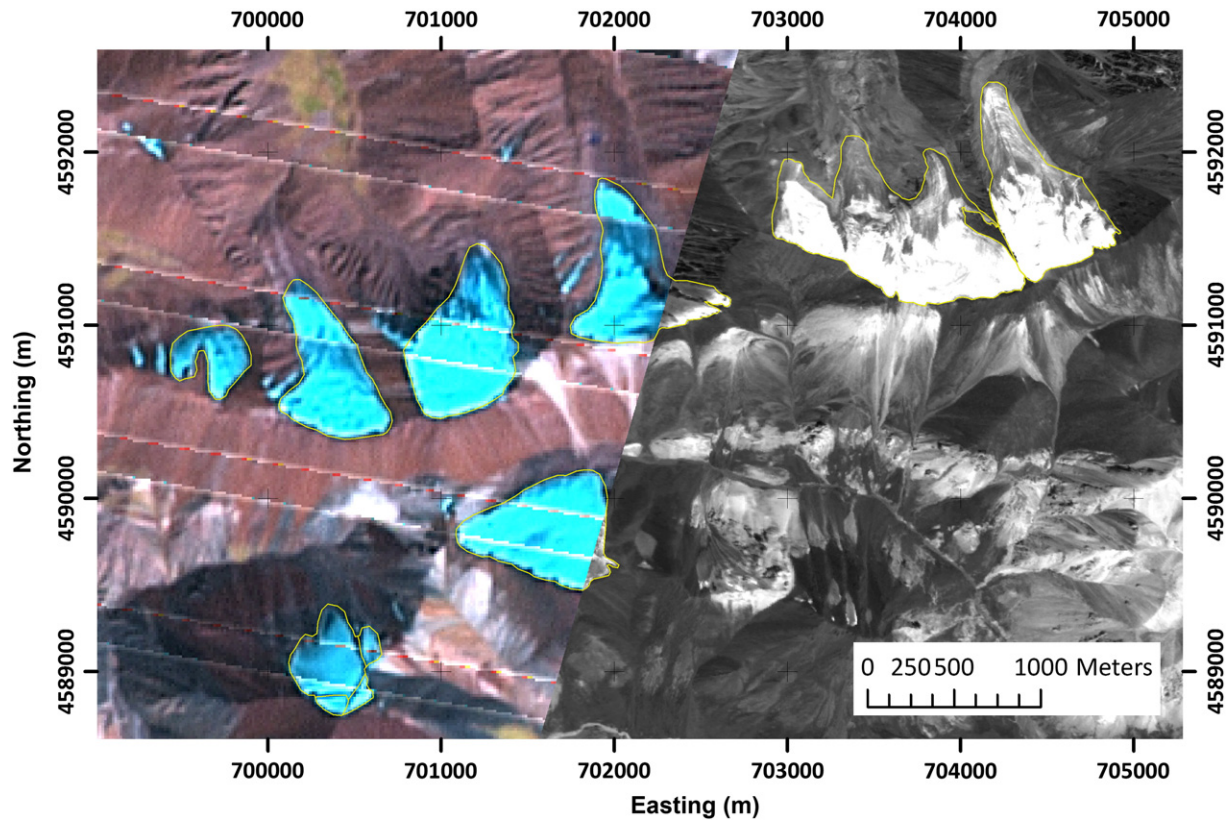
Fig. 3. Glacier outlines 2007 (yellow), mapped on the Landsat (left) and SPOT (right) images. On the Landsat image, the narrow bands between the bright stripes are the data gaps caused by the scan line corrector failure and filled by a 2008 Landsat scene. (For interpretation of the references to color in this figure legend, the reader is referred to the web version of this article.)
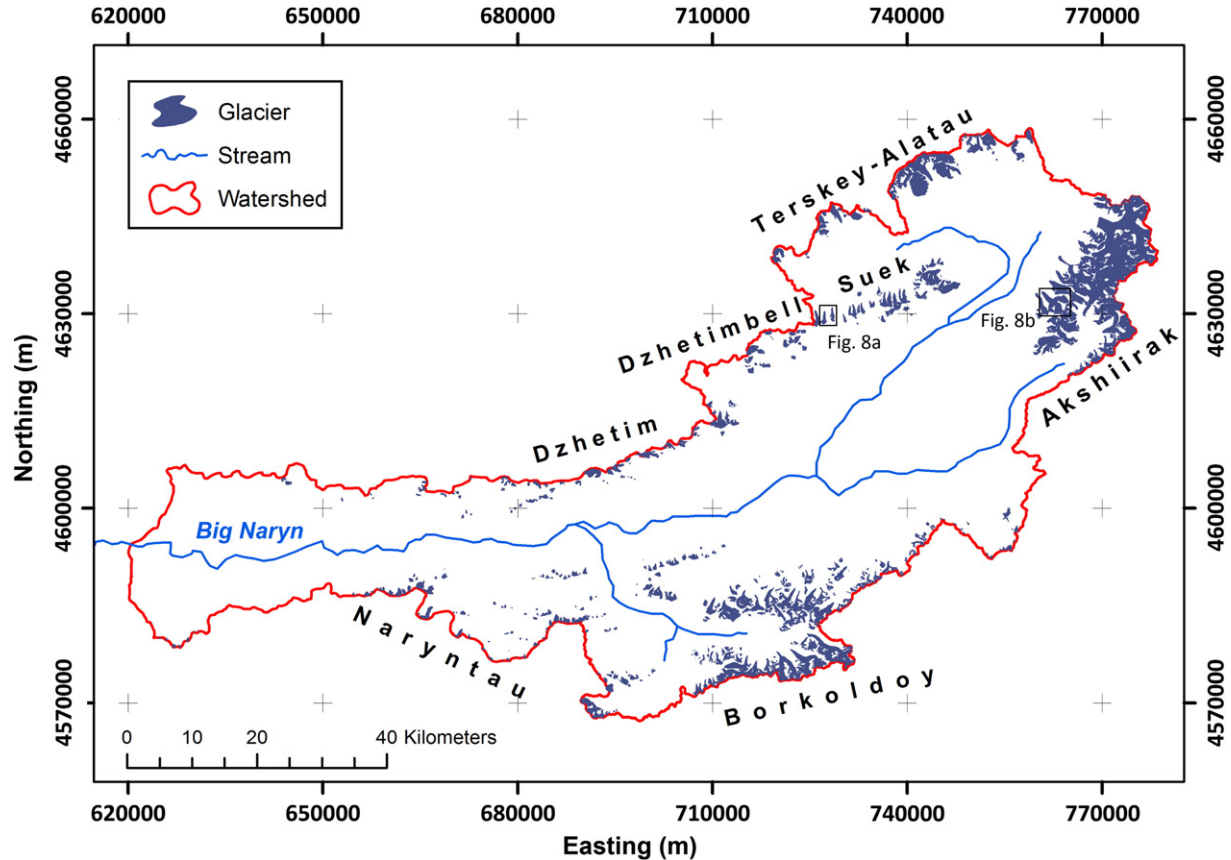

Fig. 4. Glacierized areas of the Big Naryn basin 2007, mapped from satellite imagery (Landsat, SPOT). (For interpretation of the references to color in this figure legend, the reader is referred to the web version of this article.)

(Jansson et al., 2000). From the Gregoriev ice cap, there is also evidence of cold conditions from ice core drilling (Thompson et al., 1993). Glaciers which are restricted in their lateral extent by topography require the application of a shape factor. We used a value of 0.8 as suggested by Nye (1965) for valley glaciers with elliptic cross-sections and a ratio of 3 between half-width and thickness on the centerline. This ratio was confirmed by our measurements.

Assuming a constant value over the whole glacier (Nye, 1952), the basal shear stress for the upper parts was estimated on the lower parts, where ice thickness is known from the GPR measurements (see Section 4.3). Ice thickness for the upper parts can then be calculated from the slope of the glacier surface, derived from ASTER GDEM. Similar to other studies (e.g. Farinotti et al., 2009), we determined the thicknesses along centerlines which were manually digitized for individual glacier branches by starting at the glacier snout and crossing all contours in a 90° angle. For this purpose, the slope was determined in flow direction along the centerlines. To avoid influences of small scale surface structures on the ice thickness, the slope calculation was done over a horizontal distance of 180 m at glacier No. 354 and 150 m at the two smaller glaciers. At one location on the tongue of glacier No. 354, the very small slope caused an unrealistically high ice thickness. For this point, we restricted ice thickness to a maximum value of 200 m. This limit was estimated by extending the lower valley slopes, assuming a V shape and no significant overdeepening.

The ice thickness was interpolated between the points along the flowlines and the glacier boundaries (thickness = 0) using topo2raster.

We calculated the ice volume for the whole basin using a power law which relates glacier volume to surface area (Bahr, 1997):

$$V = kS^\gamma \tag{2}$$

where: V, glacier volume (m³); k, constant of proportionality (m³⁻²ᵞ); S, glacier area (m²); and γ, scaling exponent.

We used the glacier volumes of our three test glaciers to determine the exponent γ in Eq. (2). The mean γ value was compared with values reported in the literature and volume–area scaling was used to calculate ice volumes for both inventories.

4. Results and discussion

4.1. Glacier inventory 2007

A total of 507 glaciers with an area of 471 km² has been identified and mapped on the satellite imagery (Fig. 4), corresponding to a glacierization of 8.5%.

The vast majority of glaciers (83%) is smaller than 1 km². These glaciers contain more than a quarter of the total area, which is a common picture in mountains of the mid-latitudes. In the Altay, they contribute to 86% of glacier number and 40% of glacier area, whereas in the Caucasus the corresponding numbers are 79% and 24% (after data from NSIDC, 1999). Percentage of glacier number and area quickly decrease with increasing size class (Fig. 5). There are fewer glaciers between 5 and 10 km² than between 4 and 5 km², but their total area is higher. Only 9 glaciers (1.8%) are larger than 10 km², but they contribute to 28% of the basins' ice cover. The importance of this size class is due to the plateau type glacierization of parts of the Akshiirak massif and some so called flat-summit glaciers (Avsuk, 1950) of the Terskey-Alatau (e.g. Gregoriev Glacier).

In Table 1, glacier areas and their topographic characteristics are listed for the individual mountain ranges as for 2007.

The glaciers are situated on elevations between 3700 and 5100 m a.s.l.; above 4200 m a.s.l., more than half of the catchment is glaciated. The largest areas can be found between 4200 and 4400 m a.s.l. and the majority is concentrated in the Akshiirak and Borkoldoy ranges (Fig. 6).

The distribution of glacier aspect was determined using ASTER-GDEM and shows significant differences between individual regions (Fig. 7).

In the ranges stretching west–east, the dominating orientation is north in most cases. In the Tersey Ala-Too, only the southern slope belongs to the catchment and some flat ice caps are facing east, explaining the dominance of these orientations here. The Dhzetim range is the eastern end of a mountain ridge and has a considerable fraction of glacier area with an eastern aspect. From the Akshiirak massif, only the western part which belongs to the Naryn catchment is considered in this study. Therefore, orientations from northwest to southwest play an important role here.

4.2. Changes in number and area

In the Katalog Lednikov, 700 glaciers are listed, which means a loss of 193 glaciers (28%) until 2007. 151 glaciers smaller than 0.1 km² are treated as a bulk sample in the Katalog Lednikov, without information about their location. We identified 27 glaciers which could not be found on the schematic maps of the Katalog, suggesting that they are remnants of those glaciers which were already <0.1 km² by the middle of the 20th century. The remaining 124 small glaciers could not be found again. This also means that 69 glaciers >0.1 km² must have disappeared to explain the total loss of 193 glaciers. The current glacier inventory contains 108 glaciers<0.1 km², 88 of which were still above this threshold in the 1950s. Errors in the Katalog Lednikov can also be the cause for the high number of extinct glaciers. A wrong classification of small snow patches as glaciers would easily explain an overestimation of changes in glacier number. Since the glacier mapping of the old inventory is neither
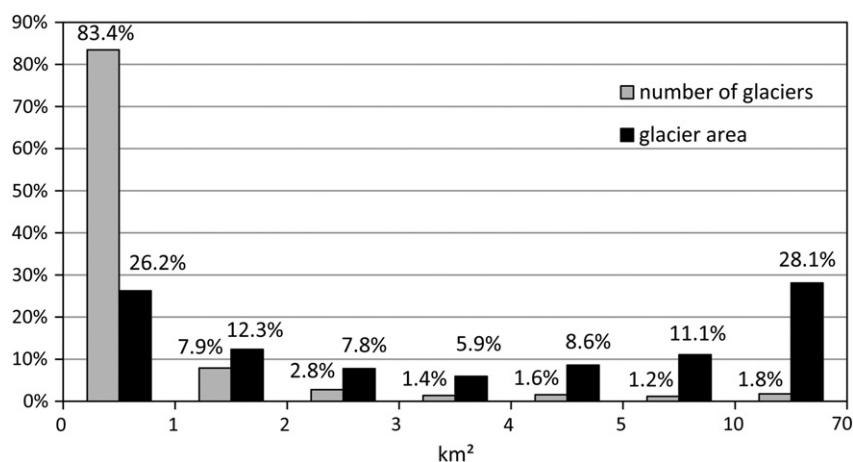

Fig. 5. Percentage of glacier number and area in different size classes. Note that the classification has no equal bin sizes.

Table 1
Number, area and topographic features of glaciers in the Big Naryn basin 2007.

Mountain range	Number of glaciers	Glacier area (km²)	Mean glacier size (km²)	Mean slope (°)	Min. elevation (m a.s.l.)	Max. elevation (m a.s.l.)	Mean elevation (m a.s.l.)	Southern orientation (%)
Akshiirak	45	181.3	4	15.6	3727	4953	4327	29.3
Borkoldoy	178	141.1	0.8	22.4	3707	5112	4342	12.3
Terskey Alatau	39	54.2	1.4	15.5	3823	4755	4290	46.5
Suek	44	30.9	0.7	17.8	3900	4582	4226	6.2
Naryntau	113	27.2	0.2	25.7	3989	4626	4277	1.9
Dzhetim	60	19.9	0.3	21.4	4029	4896	4360	39.0
Dzhetimbell	28	16.1	0.6	20.3	3800	4556	4224	8.0
Big Naryn	**507**	**470.6**	**0.9**	**17.9**	**3707**	**5112**	**4316**	**23.1%**

documented in detail nor reproducible, this possibility cannot be validated. In other studies (Bolch and Marchenko, 2009; Shahgedanova et al., 2010), where original photographs of the Katalog Lednikov were available, authors have re-mapped glacier areas and discovered differences between their results and the Katalog of around 5%. However, this value highly depends on the quality of the images, on the operator and on the extent of supraglacial debris covers (Shahgedanova et al., 2010) and therefore is not necessarily representative for the entire Katalog Lednikov.

Howsoever, assuming that all glaciers below 0.1 km² were mapped wrongly yields a maximum total error in glacier area of only 2.5%, which is negligible for our study.

The Katalog Lednikov lists a total area of 615 km² in the catchment of the Big Naryn. Until 2007, the area retreat equals −23.4%. Results for the individual mountain ranges are listed in Table 2.

The area retreat of −14% in the Akshiirak massif is in good agreement with the results of Aizen et al. (2006). They considered the Akshiirak massif as a whole, including the eastern part belonging to the Tarim basin and report an area change of −12.5% from 1943 to 2003.

Narama et al. (2006) have studied glacier area changes in the Terskey-Alatau from satellite images, but neither their investigation area nor their time span is comparable with our study. They cover a part of the range which is west of our study area and compare a Landsat image from 2002 with a Corona image from 1971. Between those dates, the mean areal retreat is 7.3% (0.20%/yr) and 8.5% (0.24%/yr) on the northern and southern slopes, respectively (Narama et al., 2006). Compared to the retreat rate of 0.68%/yr found in our study, the shrinkage documented by Narama et al. (2006) was very moderate. Kutuzov and

Shahgedanova (2009) mapped 109 glaciers of the eastern Terskey-Alatau (northern and southern slope) from 1:25,000 maps (year 1965) and Landsat and ASTER imagery (year 2003). The area decrease between these dates was 12.6%, the rate of 0.33%/yr is a little higher than the results of Narama et al. (2006), but only half of the value we have observed.

The overall area loss is approximately one quarter. However, four regions deviate considerably from this value: Akshiirak, Terskey-Alatau, Naryntau and Dzhetimbell. The lowest shrinkage is observed in the Akshiirak massif, which is due to the strong glacierization in this area. The mean glacier size is 4 km² and these large glaciers have longer response times than the considerably smaller ones in the other ranges. Therefore these react in a more delayed manner to climate fluctuations. The strong area retreat on Terskey-Alatau can be explained with the large fraction of southern orientations (47%, see table 1). Shortwave radiation is by far the most important energy source for continental glaciers. For a given relative increase in global irradiance, the highest absolute increase in shortwave radiation is found on those areas with the highest radiation sums. Therefore, southern orientations receive the highest energy surplus and react with the strongest increase in ablation. Glaciers in the Naryntau were affected by the most severe changes in area. This subregion contains the largest fraction of small and steep glaciers, inducing a quick response of glacier to climatic changes (Oerlemans, 2007). In addition, surrounding rock walls emit longwave radiation (Brazel and Marcus, 1987), which is an important energy source for small cirque glaciers (Olyphant, 1986) which are numerous in this mountain range. The Dzhetimbell range also experienced an above average area loss, which can be attributed to the relatively low elevation of
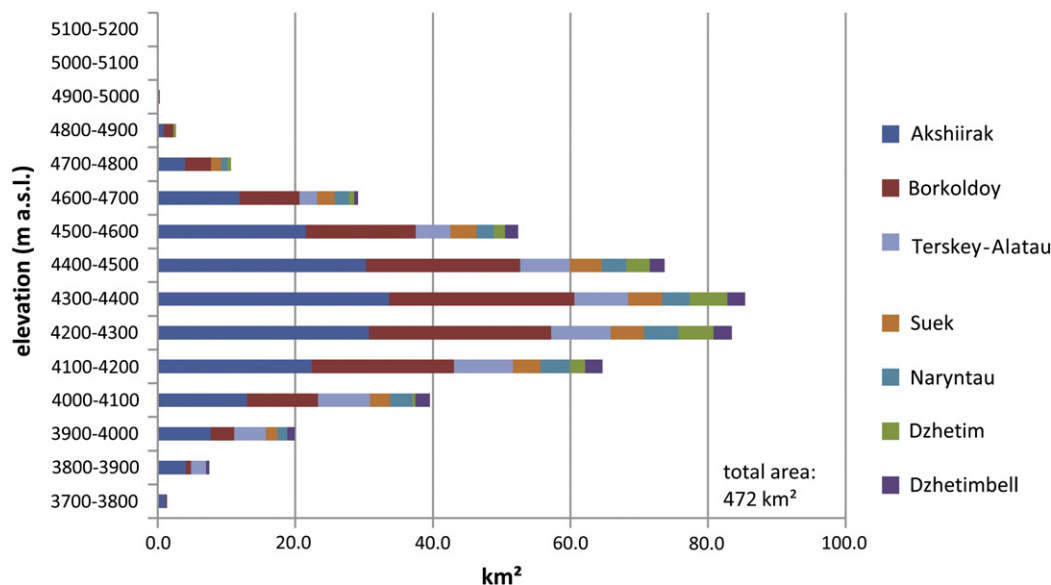

Fig. 6. Distribution of glacier area by altitude, subdivided into mountain ranges. (For interpretation of the references to color in this figure legend, the reader is referred to the web version of this article.)
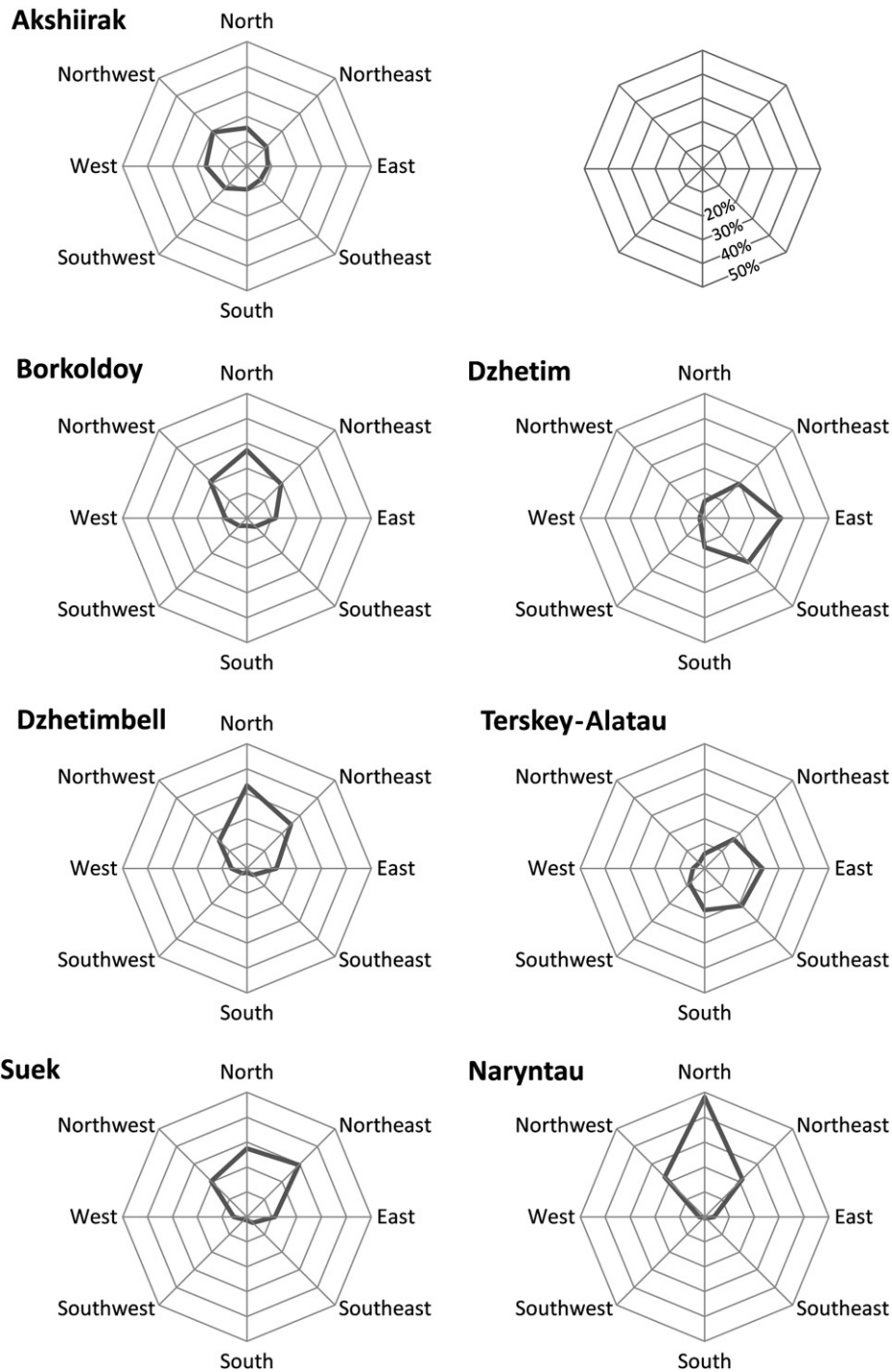
Fig. 7. Distribution of glacier area by orientation classes.

Table 2
Glacier areas listed in the Soviet Catalogue of Glaciers (mid 20th century) and in the 2007 inventory. Since the observation date in the Katalog Lednikov is not consistent (Ak-Shiirak: 1943, rest: 1956), area retreat is also given as a rate.

	Katalog Lednikov area (km²)	2007 area (km²)	Area loss (%)	Area loss (%/yr)
Akshiirak	210.9	181.3	−14.0	−0.2
Borkoldoy	185.2	141.1	−23.8	−0.5
Terskey Alatau	82	54.2	−33.9	−0.7
Suek	38.5	30.9	−19.8	−0.4
Naryntau	46.9	27.2	−42.1	−0.8
Dzhetim	27.6	19.9	−28.0	−0.6
Dzhetimbell	23.4	16.1	−31.4	−0.6
Big Naryn	**614.5**	**470.6**	**−23.4**	−

the glaciers, which reach a maximum of 4556 m a.s.l. (Table 1), the lowest value for all regions. Therefore, the equilibrium lines reach the uppermost parts of the glaciers sooner than elsewhere. This leads to very small accumulation areas compared to ablation areas and consequently to very negative mass balances.

4.3. Determination of glacier volumes

The profiles of the GPR measurements and the interpolated ice thicknesses are displayed in Fig. 8. As expected, the glacier tongues are situated in rather regular valley troughs with a continuous increase of ice thickness along the central flow line.
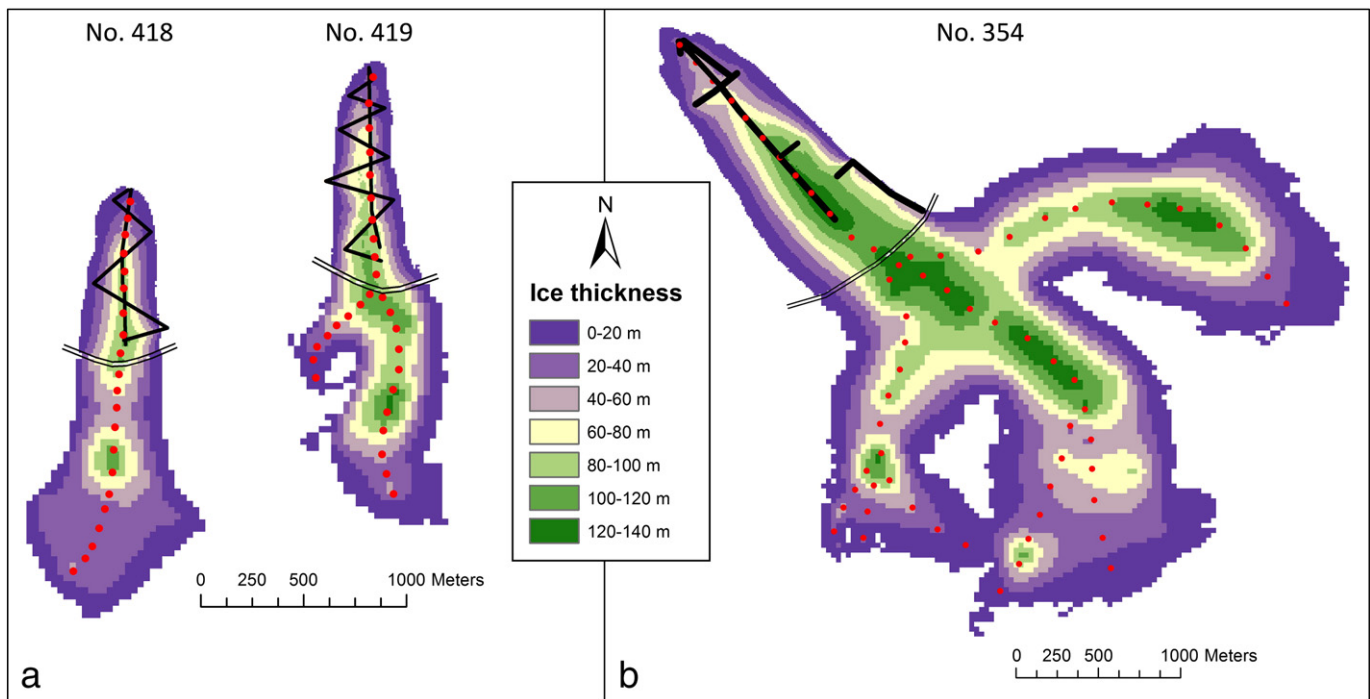
Fig. 8. Ice thicknesses determined on glaciers Nos. 418 and 419 in the Suek range and No. 354 in the Akshiirak massif. The thick black lines are the tracks of the GPR measurements. Upstream of the thin double lines, ice thicknesses were determined from the surface slope along the central flowlines (red dots) and interpolated to the glacier margins. (For interpretation of the references to color in this figure legend, the reader is referred to the web version of this article.)

The volumes of the lower glacier parts were determined from the interpolated ice thicknesses distribution. The basal shear stress along the central flowlines was calculated using Eq. (1), the mean values are 100 kPa, 110 kPa and 150 kPa for the glaciers Nos. 354, 418 and 419, respectively. Using these values in Eq. (1) enabled us to derive ice thicknesses along the flowlines of the upper parts, which were interpolated to the glacier boundaries. The ice thicknesses determined by GPR measurements and by calculations from the surface slope match very well along the central flowlines of the three glaciers (Fig 9). The sum of the lower (measured) and upper (calculated) glacier parts gives total volumes of the three glaciers of 272 Mil. m³ (No. 354), 27 Mil. m³ (No. 418) and 33 Mil. m³ (No. 419).

To assess the sensitivity of the basal shear stress (τ), we varied the values derived on the glacier tongues by $\pm 10\%$. The resulting deviations of the total glacier volumes are $\pm 6.5\%$ (Nos. 418 and 419) and $\pm 8.0\%$ (No. 354). Glacier No. 354 shows the strongest sensitivity to variations of τ, because here, the upper part on which ice thickness is calculated has the largest share in total glacier area.

The vertical section demonstrates that, according to the principles of ice flow, the steeper glacier parts are relatively thin and that the majority of the ice volume is stored in the lower, flatter parts. Slope is very sensitive for the calculation of ice thicknesses. Even very gentle variations of the surface slope produce distinct bumps in the glacier bed (Fig. 9). Although the calculated bedrock in Fig. 9 is slightly smoothed using a spline function, the bedrock determined by GPR measurements appears somewhat smoother, but the mean ice thicknesses of the two methods agree very well. The only severe divergence is in the lowermost parts, where basal shear stress goes towards zero. It is obvious that at the glacier snout, calculation of ice thickness from surface slope is impossible.

4.4. Volume–area-scaling

Bahr (1997) used a probability-density function for the constant k determined on 144 glaciers and found the mean of the distribution to be 0.191 $m^{3-2\gamma}$. Since the exponent (γ) is the most sensitive parameter

of the scaling relation, we want to determine its value for the three test glaciers. Using a constant k of 0.191 $m^{3-2\gamma}$ in Eq. (2) requires exponents (γ) of 1.352 (No. 354), 1.378 (No. 418) and 1.396 (No. 419) to describe the volume–area relation of the three glaciers. The mean γ of 1.375 is identical to the value Bahr (1997) derived by theoretical considerations. An analysis of the volumes and areas of 63 glaciers listed by Chen and Ohmura (1990) shows that the variation of γ is large. Assuming the constant k to be 0.191 $m^{3-2\gamma}$, the exponent γ varies from 1.28 to 1.42, with an average value of 1.36 and a standard deviation of 0.018. This variability shows that the mean value derived from our small sample might not be representative for the region. For this reason, we also apply the γ of 1.36 which was found in worldwide datasets (Chen and Ohmura, 1990; Meier and Bahr, 1996). The resulting ice volumes for the two inventories and the changes between them are listed in Table 3.

The 2007 ice volume calculated with a γ of 1.375 is 33.3 km². This is 28% above the total volume resulting from a γ value of 1.36. The same relative discrepancies occur when the two exponents are used in scaling the data from the Katalog Lednikov. The resulting volume loss is 6.6–8.4 km³ while the relative loss is 20% for both values of γ.

The power relationships found by Macheret et al. (1988) in the Dzhungarian Alatau cannot be directly compared to our entire investigation area, because they excluded glaciers smaller than 0.1 km² and flat-summit glaciers. Moreover, they used two different equations for valley glaciers and cirque glaciers.

Assuming a mean density of glacier ice of 910 kg/m³ (Paterson, 1994), the glacier volume loss of 3.1–4.0 km³ in the Akshiirak massif is equivalent to 3.0–3.86 km³ of water. Evaporation and sublimation are difficult to quantify due to the lack of observational data. According to Cicenko (1966), evaporation is balanced by condensation on glaciers in the Central Tian Shan. If we assume that all the ablation was due to melting processes, the ice loss in the Akshiirak massif contributed to 3.0–3.8% of total discharge in the Big Naryn basin from 1943 to 2007. This value is only the non-steady contribution from the volume loss. The remaining volume loss in the other mountain ranges of 3.5–4.4 km³ (3.2–4.0 km³ water equivalent) is
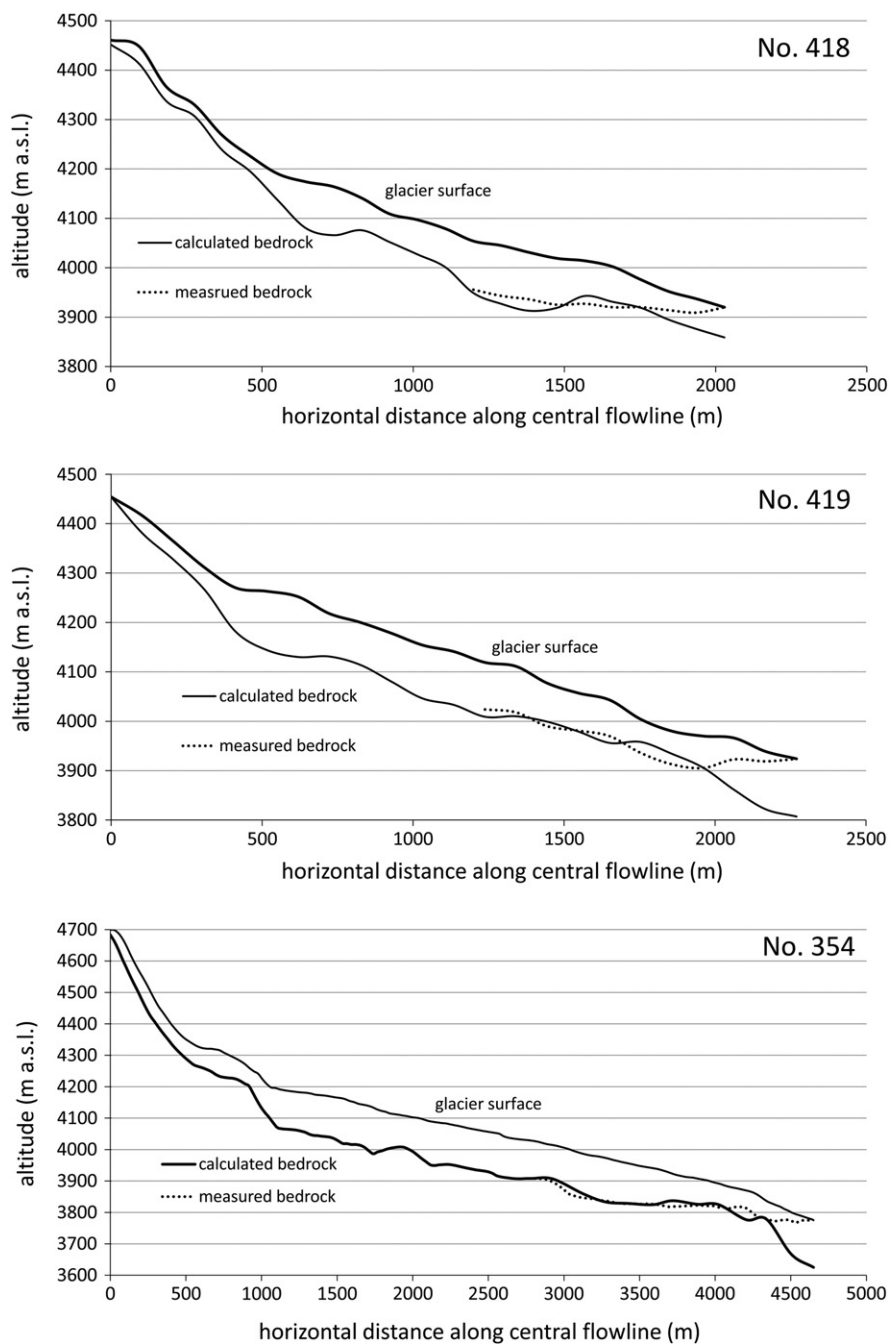
Fig. 9. Longitudinal profile of glacier surface and bedrock along the central flowlines. Ice thickness was calculated from surface slope considering a simplified ice mechanical approach. On the glacier tongues, it was additionally measured by ground penetrating radar. Final ice volumes were calculated from measured thicknesses on the lower parts and calculated thicknesses from the upper parts.

related to the period between 1956 and 2007 and has a share of 4.3–5.4% in total runoff volume. These percentages sum up to a total of 7.3–9.2%, but they are related to different periods. Since the years 1943–1955, which are only considered in the Akshiirak data, were comparably cool and wet (Fig. 2), the total percentage can be regarded as a minimum for the past 50 yr (1956–2007). For comparison, the Ziller catchment at Mayrhofen in the Austrian Alps has a glacierization similar to the Big Naryn and here, the areal retreat of 19.8% from 1969 to 1999 caused an additional runoff which contributed to 2% of the discharge volume (Lambrecht and Mayer, 2009). The significantly higher fraction in the Big Naryn basin is certainly due to the continental climate. In dryer regions, it takes longer for large glaciers to develop and to turn over their mass (Oerlemans,

2007). A release of water due to the reduction of the storage volume has more impact in an arid climate, because here, this hydrological signal is to a lesser degree modified by rainfall (Kaser et al., 2010).

5. Conclusion

The differences in glacier area recession between the individual mountain groups suggest that the retreat rate of glaciers in the Big Naryn basin is not controlled by a single cause, but by the interaction of several causes. In some cases, dominating parameters can be identified easily, in others it seems more difficult to explain the area loss. An important driver which was completely excluded from this study due to the lack of observational data is the spatial variability of

Table 3

Ice volumes and their relative changes derived by volume–area scaling for the individual ranges of the Big Naryn basin for the Katalog Lednikov (Akshiirak: 1943, rest: 1956) and for the 2007 inventory. Volume (V) was calculated from area (S) using the formulation $V = 0.191 S^\gamma$. The γ of 1.375 was derived theoretically by Bahr (1997) and confirmed by volume determinations on three glaciers (this study), the γ of 1.36 is the mean value found in worldwide datasets (Chen and Ohmura, 1990; Meier and Bahr, 1996).

	$\gamma = 1.375$			$\gamma = 1.36$		
	Volume Katalog Lednikov (km^3)	Volume 2007 (km^3)	Volume changes (%)	Volume Katalog Lednikov (km^3)	Volume 2007 (km^3)	Volume changes (%)
Akshiirak	24.6	20.6	−16.3	19.0	15.9	−16.2
Borkoldoy	8.8	6.9	−21.9	7.0	5.5	−21.8
Terskey Alatau	4.3	2.8	−33.7	3.4	2.2	−33.5
Suek	1.3	1.2	−12.1	1.1	1.0	−12.3
Naryntau	1.1	0.7	−34.4	0.9	0.6	−34.4
Dzhetim	0.9	0.6	−36.6	0.7	0.5	−36.4
Dzhetimbell	0.7	0.6	−24.0	0.6	0.5	−23.8
Big Naryn	**41.7**	**33.3**	**−20.2**	**32.6**	**26.0**	**−20.1**

precipitation. The exposition to moist air masses and dominating wind directions are strongly controlling the equilibrium line altitude on glaciers (Maisch et al., 2000).

We used ice thickness measurements and a simplified ice mechanical approach to determine the volumes of three glaciers. Power law relations between glacier volume and area were applied to estimate recent and past ice volumes. The knowledge of ice volume loss in the past decades will serve to calibrate hydrological models and the knowledge of the current ice volume is an important prerequisite for future scenarios of water availability in the headwater of Syr-Darya river.

Although since 1943, annual precipitation decreased with a rate of 21 mm per decade, annual discharge in the Big Naryn basin slightly increased by 3.7 mm per decade. This is due to the excess water provided by glacier degradation, which contributed to approximately 8% of annual runoff during the second half of the 20th century.

Acknowledgements

Appendix A. Supplementary data

Supplementary data associated with this article can be found in the online version, at http://dx.doi.org/10.1016/j.gloplacha.2012.07.010. These data include Google maps of the most important areas described in this article.

References

Aizen, V., Kuzmichenok, V.A., Surazakov, A.B., Aizen, E.M., 2006. Glacier changes in central and northern Tien Shan during the last 140 years based on surface and remote sensing data. Annals of Glaciology 43, 202–213.

Aizen, V.B., Kuzmichenok, V.A., Surazakov, A.B., Aizen, E.M., 2007. Glacier changes in the Tien Shan as determined from topographic and remotely sensed data. Global and Planetary Change 56, 328–340.

Allouche, J., 2007. The governance of Central Asian waters: national interests versus regional cooperation. Disarmament Forum 2007 (4), 45–56.

Anon., 1977. Katalog Lednikov SSSR (Catalogue of Glaciers of the USSR), vol. 14. Gidrometeoizdat, Leningrad (in Russian).

Avsuk, G.A., 1950. Ledniki ploskih vershyn (Flat summit glaciers). Trudy Instituta Geografii (Proceedings of the Institute of Geography) 5, 15–44 (in Russian).

Bahr, D.B., 1997. Global distributions of glacier properties: a stochastic scaling paradigm. Water Resources Research 33, 1669–1679.

Bolch, T., 2007. Climate change and glacier retreat in northern Tien Shan (Kazakhstan/Kyrgyzstan) using remote sensing data. Global and Planetary Change 56, 1–12.

Bolch, T., Kamp, U., 2006. Glacier mapping in high mountains using DEMs, Landsat and ASTER data. Proceedings of the 8th International Symposium on High Mountain Remote Sensing Cartography, 20–27 March 2005, La Paz, Bolivia: Grazer Schriften der Geographie und Raumforschung, 41, pp. 13–24.

Bolch, T., Marchenko, S.S., 2009. Significance of glaciers, rockglaciers and ice rich permafrost in the Northern Tien Shan as water towers under climate change conditions. In: Braun, L., Hagg, W., Severskiy, I., Young, G. (Eds.), Assessment of Snow, Glacier and Water Resources in Asia, IHP/HWRP Berichte, 8, pp. 132–144.

Bolch, T., Menounos, B., Wheate, R., 2010. Landsat-based inventory of glaciers in western Canada, 1985–2005. Remote Sensing of Environment 114, 127–137.

Brazel, A.J., Marcus, M.G., 1987. Heat enhancement by longwave wall emittance. Geographical Review 77, 440–455.

Chen, J., Ohmura, A., 1990. Estimation of Alpine glacier water resources and their change since the 1870s. IAHS Publications 193, 127–135.

Cicenko, K.V., 1966. K raschetu stoka s vysotnyh zon gornyh basseynov (About calculation of runoff from altitude zones of mountain basins). In: Atakanov, U.A., Sadivakas, U. (Eds.), Voprosy geografii Kirgizii (Questions of Kirghizkiy Geography). Ilim Publishing, Frunze, pp. 62–63 (in Russian).

ECE, 2011. Second assessment of transboundary rivers, lakes and groundwaters. Economic Commission for Europe, Convention on the Protection and Use of Transboundary Watercourses and International Lakes. United Nations, New York and Geneva.

Erasov, N.V., 1968. Metod opredeleniya obyoma gornyh lednikov (Method to determine the volume of mountain glaciers). Data of Glaciological Studies 14, 307–308 (in Russian).

Farinotti, D., Huss, M., Bauder, A., Funk, M., Truffer, M., 2009. A method for estimating the ice volume and ice thickness distribution of alpine glaciers. Journal of Glaciology 191, 422–430.

Fujita, K., Takeuchi, N., Nikitin, S.A., Surazakov, A.B., Okamoto, S., Aizen, V.B., Kubota, J., 2011. Favorable climatic regime for maintaining the present-day geometry of the Gregoriev Glacier, Inner Tien Shan. The Cryosphere 5, 539–549.

Haeberli, W., Hoelzle, M., 1995. Application of inventory data for estimating characteristics of and regional climate change effects on mountain glaciers: a pilot study with the European Alps. Annals of Glaciology 21, 206–212.

Hutchinson, M.F., 1993. Development of a continent-wide DEM with applications to terrain and climate analysis. In: Goodchild, M.F., Steyaert, L.T., Parks, B.O., Johnston, C. (Eds.), Environmental Modeling with GIS, 392–399. Oxford University Press, New York, pp. 392–399.

IPCC, 2007. Summary for policymakers. In: Solomon, S., Qin, D., Manning, M., Chen, Z., Marquis, M., Averyt, K.B., Tignor, M., Miller, H.L. (Eds.), Climate Change 2007: The Physical Science Basis. : Contribution of Working Group I to the Fourth Assessment Report of the Intergovernmental Panel on Climate Change. Cambridge University Press, Cambridge, United Kingdom and New York, NY, USA.

Jansson, P., Näslund, J.-O., Pettersson, R., Richardson-Näslund, C., Holmlund, P., 2000. Debris entrainment and polythermal structure in the terminus of Storglaciären. IAHS Publications 264, 143–151.

Kaser, G., Großhauser, M., Marzeion, B., 2010. Contribution potential of glaciers to water availability in different climate regimes. Proceedings of the National Academy of Sciences of the United States of America 107, 20223–20227.

Kendall, M.G., 1975. Rank Correlation Methods. Griffin, London.

Kutuzov, S., Shahgedanova, M., 2009. Glacier retreat and climatic variability in the eastern Terskey-Alatoo, inner Tien Shan between the middle of the 19th century and beginning of the 21st century. Global and Planetary Change 69, 59–70.

Lambrecht, A., Mayer, C., 2009. Temporal variability of the non-steady contribution from glaciers to water discharge in western Austria. Journal of Hydrology 376, 353–361.

Li, B., Zhu, A., Zhang, Y., Pei, T., Qin, C., Zhou, C., 2007. Glacier change over the past four decades in the middle Chinese Tien Shan. Journal of Glaciology 52, 425–432.

Linsbauer, A., Paul, F., Hoelzle, M., Frey, H., Haeberli, W., 2009. The Swiss Alps without glaciers — a GIS-based modelling approach for reconstruction of glacier beds. Proceedings of Geomorphometry 2009. Zurich, Switzerland, pp. 243–247.

Liu, S., Ding, Y., Shangguan, D., Zhang, Y., Li, J., Han, H., Wang, J., Xie, C., 2006. Glacier retreat as a result of climate warming and increased precipitation in the Tarim river basin, northwest China. Annals of Glaciology 43, 91–96.

Macheret, Y., Cherkasov, P.A., Bobrova, L.I., 1988. The thickness and volume of Dzhungarskiy Alatau glaciers from airborne radio echo-sounding data. Data of Glaciological Studies 62, 59–70 (in Russian).

Maisch, M., Wipf, A., Denneler, B., Battaglia, J., Benz, C., 2000. Die Gletscher der Schweizer Alpen. Gletscherhochstand 1850, Aktuelle Vergletscherung, Gletscherschwund-Szenarien (Glaciers of the Swiss Alps. Glacier Extent 1850, Recent Glacierization, Deglacierization Scenarios). vdf Hochschulverlag, Zurich. (in German).

Meier, M.F., Bahr, D.B., 1996. Counting glaciers: use of scaling methods to estimate the number and size distribution of the glaciers of the world. In: Colbeck, S.C. (Ed.), Glaciers, Ice Sheets and Volcanoes: A Tribute to Mark F. Meier: CRREL Special Report, vol. 96–27, pp. 89–94.

Narama, C., Shimamura, Y., Nakayama, D., Abdrakhmatov, K., 2006. Recent changes of glacier coverage in the western Terskey-Alatoo range, Kyrgyz Republic, using Corona and Landsat. Annals of Glaciology 43, 223–229.

Narama, C., Kääb, A., Duishonakunov, M., Abdrakhmatov, K., 2009. Spatial variability of recent glacier area changes in the Tien Shan Mountains, Central Asia, using Corona (1970), Landsat (2000), and ALOS (2007) satellite data. Global and Planetary Change 71, 42–54.

NSIDC, 1999. World Glacier Inventory. National Snow & Ice Data Center, Boulder, CO.

Nye, J.F., 1952. The mechanics of glacier flow. Journal of Glaciology 2, 82–93.

Nye, J.F., 1965. The flow of a glacier in a channel of rectangular, elliptic or parabolic cross-section. Journal of Glaciology 41, 661–690.

Oerlemans, J., 2007. Estimating response times of Vadret da Morteratsch, Vadret da Palü, Briksdalsbreen and Nigardsbreen from their length records. Journal of Glaciology 182, 357–362.

Olyphant, G.A., 1986. Longwave radiation in mountainous areas and its influence on the energy balance of Alpine snowfields. Water Resources Research 22, 62–66.

Paterson, W.S.B., 1994. The Physics of Glaciers, 3 edition. Butterworth-Heinemann. 496 pp.

Paul, F., Kääb, A., 2005. Perspectives on the production of a glacier inventory from multispectral satellite data in Arctic Canada: Cumberland Peninsula, Baffin Island. Annals of Glaciology 42, 59–66.

Radić, V., Hock, R., 2010. Regional and global volumes of glaciers derived from statistical upscaling of glacier inventory data. Journal of Geophysical Research 115, F01010.

Radić, V., Hock, R., Oerlemans, J., 2007. Volume–area scaling vs flowline modelling in glacier volume projections. Annals of Glaciology 46, 234–240.

Radić, V., Hock, R., Oerlemans, J., 2008. Analysis of scaling methods in deriving future volume evolutions of valley glaciers. Journal of Glaciology 178, 601–612.

Raper, S.C.B., Braithwaite, R., 2006. Low sea level rise projections from mountain glaciers and icecaps under global warming. Nature 439, 311–313.

Sen, P.K., 1968. Estimates of the regression coefficient based in Kendall's tau. Journal of the American Statistical Association 63, 1379–1389.

Shahgedanova, M., Nosenko, G., Khromova, T., Muraveyev, A., 2010. Glacier shrinkage and climatic change in the Russian Altai from the mid 20th century: an assessment using remote sensing and PRECIS regional climate model. Journal of Geophysical Research 115, D16107.

Thompson, L.G., Mosley-Thompson, E., Davis, M., Lin, P.N., Yao, T., Dyurgerov, M., Dai, J., 1993. "Recent warming": ice core evidence from tropical ice cores with emphasis on Central Asia. Global and Planetary Change 7, 145–156.

Van de Wal, R.S.W., Wild, M., 2001. Modelling the response of glaciers to climate change by applying volume–area scaling in combination with a high resolution GCM. Climate Dynamics 18, 359–366.

Weber, M., Braun, L., Mauser, W., Prasch, M., 2010. Contribution of rain, snow- and icemelt in the upper Danube discharge today and in the future. Geografia Fisica e Dinamica Quaternaria 33, 221–230.